STRESS ANALYSIS OF FILAMENT-WOUND COMPOSITE CYLINDERS UNDER COMBINED INTERNAL PRESSURE AND THERMAL LOADING

Hasan Çallıoğlu[1], Emin Ergun[1]* and Oktay Demirdağ[2]

[1]Department of Mechanical Engineering, Pamukkale University, 20020, Kınıklı,
[2]Department of Civil Engineering, Pamukkale University, 20020, Kınıklı,
Denizli, Turkey

*Author to whom correspondence should be addressed
e-mail: eminergun@pau.edu.tr

Received 17 September 2007; accepted 13 February 2008

ABSTRACT

An analytical solution is performed using stress function approach for multi-layered filament-wound composite cylinders subjected to combined internal pressure and thermal loading. It is assumed that there is a liquid or gas of various temperatures in the cylinders. The effects of the wind angle variation through the radial section of the cylinders are also investigated. Thus, the layers are oriented symmetrically and antisymmetrically for (0°/90°), (30°/-30°), (45°/-45°) and (60°/-60°) orientations. A computer program is developed to conduct stress and deformation analyses of composite cylinder with different winding angle. All the integration constants are found from the radial stress and displacement in the normal direction of layers.

Keywords: Composite cylinders, thermal stress, internal pressure, stress analysis.

1. INTRODUCTION

There is increasing demand worldwide for manufacturing cylindrical structures made of composite materials, since they can be used in a great variety of application in almost every sector of the constructional industry. Filament winding is one of the popular production techniques for composite structures. Continuous filaments are an economical and excellent form of fibre reinforcement and can be oriented to match the direction of the stress loaded in a structure. Due to many potential advantages such as high specific stiffness and strength, good corrosion resistance and thermal insulation, filament-wound structures are being used in many applications such as fuel tanks, oxidizer tanks, rocket motors, motor cases and pipes.

The general theory for the anisotropic cylinders is given in literature [1]. Rosenow [2] used the classical laminated plate theory to predict the stress and strain response of pipes with winding angles varying from 15° to 85°, and he compared his predictions with experimental results. Hyer et al. [3] investigated stresses and deformations in cross-ply composite tubes subjected to uniform temperature change. Soden et al. [4] investigated the influence of the winding on the strength and deformation of filament-wound composite tubes under uniaxial and biaxial forces. Chouchaoui and Ochoa [5] developed a general analytical model for the stress and displacements of orthotropic hollow cylinders. Recently, some studies are presented under the action of transverse loading [6], internal pressure [7] and combined centrifugal, pressure and axial loading [8]. Chen et al. [9] investigated the problem of a cylindrically anisotropic elastic circular tube subjected to pressuring, shearing, torsion, extension and a uniform temperature change. Tarn and Wang [10] presented a state space approach to extension, torsion, bending, shearing and pressuring of laminated composites tubes. Xia et al. [11] presented an exact solution for multi-layered filament-wound fibre reinforced sandwich pipes under pure bending. Xia et al. [12] presented a solution based on the classical cylindrical-plate theory for the thermal stress and strain in a filament-wound fibre-reinforced sandwich pipe subjected to internal pressure and temperature change. Liew et al. [13] presented an analysis of the thermomechanical behaviour of hollow circular cylinders of functionally graded material. Sayman [14] presented a general stress method for thick and thin multilayered composite cylinders un-

der hygrothermal loadings. Parnas and Katırcı [15] developed an analytical procedure in order to design and predict the behaviour of fibre reinforced composite pressure vessels under internal pressure, axial force, body force, and temperature and moisture variation. Beakou and Mohamed [16] investigated numerically the influence of the scattering of design variables (strengths, constituent elastic constants, load cases, etc.) on the optimal fibre winding angle of cylindrical laminated composites. Kaddour et al. [17] presented the experimental results describing in detail the behaviour of tubes, of various wall thicknesses, under combined internal pressure and axial compression. Mistry et al. [18] studied the collapse behaviour of filament-wound glass fibre/epoxy cylinders both experimentally and theoretically under combinations of external pressure and axial loading in the third quadrant of the stress plane. Tarakçıoğlu et al. [19] investigated the effect of surface cracks on strength theoretically and experimentally for glass/epoxy filament wound pipes. Çallıoğlu [20] studied stress analysis on a rotating hollow disc of rectilinearly glass-fibre/epoxy prepreg under thermal loading.

In the study, a stress analysis is developed for the multi-layered thin or thick composite cylinders under combined internal pressure and temperature loading. The solution is carried out for plane-strain case. It is supposed that the temperature's distribution is linear across the thickness. In the case of internal pressure solely, results obtained are compared with those in the literature. The effects of the wind angle variation through the radial section of the cylinders are also investigated.

2. ELASTIC SOLUTION

A fibre reinforced multi-layered composite cylinder is shown in Fig. 1. *r, θ* and *z* are the radial, tangential and axial directions, respectively. The governing equilibrium equation for the axisymmetric problem is

$$r\frac{d\sigma_r}{dr}+\sigma_r-\sigma_\theta=0 \tag{1}$$

The geometric relation between strains and radial displacement for the axially symmetric cases is given by

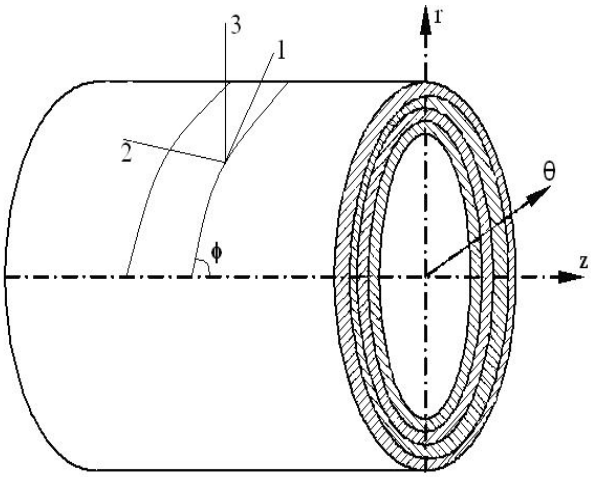

Fig. 1. A multi-layered cylinder

$$\varepsilon_r=\frac{du}{dr},\qquad \varepsilon_\theta=\frac{u}{r} \tag{2}$$

where u is the displacement component in the radial direction. The strain compatibility equation can be derived from Eq. (2) as follows:

$$r\frac{d\,\varepsilon_\theta}{dr}+\varepsilon_\theta-\varepsilon_r=0 \tag{3}$$

The stress-strain relations for each ply with polar orthotropic material are [1]

$$\begin{aligned}\varepsilon_r&=a_{rr}\sigma_r+a_{r\theta}\sigma_\theta+a_{rz}\sigma_z+\alpha_r\,\Delta T\\ \varepsilon_\theta&=a_{r\theta}\sigma_r+a_{\theta\theta}\sigma_\theta+a_{\theta z}\sigma_z+\alpha_\theta\,\Delta T\\ \varepsilon_z&=a_{rz}\sigma_r+a_{\theta z}\sigma_\theta+a_{zz}\sigma_z+\alpha_z\,\Delta T\end{aligned} \tag{4}$$

where a_{ij} are the components of the compliance matrix as $a_{rr}=\frac{1}{E_2},\quad a_{\theta\theta}=\frac{1}{E_1},\quad a_{r\theta}=-\frac{\nu_{r\theta}}{E_2}$ and E_1 and E_2 are moduli of elasticity of the radial and tangential direction. α_1 are the thermal expansion coefficients. $\Delta T=T$, T is temperature function. $\tau_{r\theta}$ is zero for polar axisymmetric cases.

For the plane-strain case, ε_z is zero, and σ_z can be written from Eq. (4) as,

$$\sigma_z=-\frac{a_{rz}}{a_{zz}}\sigma_r-\frac{a_{\theta z}}{a_{zz}}\sigma_\theta-\frac{\alpha_z}{a_{zz}}T \tag{5}$$

Substituting Eq. (5) into Eq. (4) gives

$$\varepsilon_r = \beta_{rr}\sigma_r + \beta_{r\theta}\sigma_\theta + \overline{\alpha}_r T$$
$$\varepsilon_\theta = \beta_{r\theta}\sigma_r + \beta_{\theta\theta}\sigma_\theta + \overline{\alpha}_\theta T \quad (6)$$

where

$$\beta_{ij} = a_{ij} - a_{jz}\frac{a_{iz}}{a_{zz}}$$
$$\overline{\alpha}_i = \alpha_i - \alpha_z\frac{a_{iz}}{a_{zz}}$$

The equilibrium equation (1) is satisfied by the stress function F defined as

$$\sigma_r = \frac{1}{r}\frac{dF}{dr}, \qquad \sigma_\theta = \frac{d^2F}{dr^2} \quad (7)$$

From Equations (1)-(7), an ordinary differential equation for the stress function *F* emerges as,

$$r^3\frac{d^3F}{dr^3} + r^2\frac{d^2F}{dr^2} - k^2 r\frac{dF}{dr} = \frac{\overline{\alpha}_r - \overline{\alpha}_\theta}{\beta_{\theta\theta}}r^2 T - \frac{\overline{\alpha}_\theta}{\beta_{\theta\theta}}r^3\frac{dT}{dr} \quad (8)$$

where $k^2 = \dfrac{\beta_{rr}}{\beta_{\theta\theta}}$ and *T* is the temperature function considered as,

$$T = T_a - T_0 + (T_b - T_a)\frac{r-a}{b-a} \quad (9)$$

where a and b are inner and outer radii of the cylinder. T_a and T_b are, respectively, temperatures in the inner and outer surfaces, and T_o is the reference temperature.

The stress function F can be written by using the transform of $r=e^t$ as

$$F = C_0 + C_1 r^{1+k} + C_2 r^{1-k} + Ar^3 + Br^2 \quad (10)$$

where C_0, C_1 and C_2 are the integration constants and A and B terms are:

$$A = -\frac{\overline{\alpha}_\theta\left(\dfrac{T_b - T_a}{b-a}\right)}{3\beta_{\theta\theta}\left(4-k^2\right)}$$
$$B = \frac{T\left(\overline{\alpha}_r - \overline{\alpha}_\theta\right)}{2\beta_{\theta\theta}\left(1-k^2\right)} \quad (11)$$

The stress components are obtained from the stress function as,

$$\sigma_r = C_1(1+k)r^{k-1} + C_2(1-k)r^{-k-1} + 3Ar + 2B$$
$$\sigma_\theta = C_1 k(1+k)r^{k-1} - C_2 k(1-k)r^{-k-1} + 6Ar + 2B \quad (12)$$

3. RADIAL DISPLACEMENT

The radial displacement component can be found from ε_θ as

$$u = C_1(1+k)r^k(\beta_{r\theta} + k\beta_{\theta\theta}) + C_2(1-k)r^{-k}(\beta_{r\theta} - k\beta_{\theta\theta}) + \\ + 3Ar^2(\beta_{r\theta} + 2\beta_{\theta\theta}) + 2Br(\beta_{r\theta} + \beta_{\theta\theta}) + \overline{\alpha}_\theta rT \quad (13)$$

If the composite cylinder is manufactured by using n layers, the numbers of integration constants are 2×n. The number of the boundary conditions must be equal to 2×n. The cylinder is subjected to internal pressure, therefore,

$$\sigma_r = -P_i \quad at\ r = a$$
$$\sigma_r = 0 \quad at\ r = b \quad (14)$$

The radial stress component and radial displacement (They are both in the normal direction of the surface as shown in Fig. 2) must be equal at the boundaries for different layers. So, 2×n-2 more boundary conditions can be written for the radial stress and displacement. Thus, the total number of boundary conditions reaches 2×n. They are written in the matrix form and then the integration constants are obtained by using the Gauss-Jordan method. Then, the stresses and displacements in each layer can be calculated by using known integration constants.

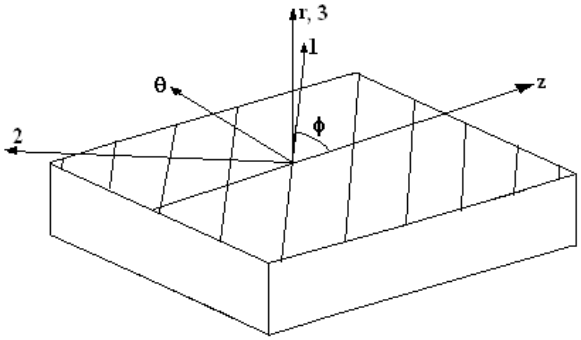

Fig. 2. Principal material directions

4. RESULTS AND DISCUSSION

Since it is assumed that there is a liquid or gas of various temperatures in the cylinders, an analytical solution is performed for multi-layered filament-wound composite cylinders subjected to combined internal pressure (Pi) and thermal loading (T). The

Table 1. Mechanical properties of a composite layer [20]

Elasticity Moduli (MPa)	E_1	26950
	E_2	21800
Shear Modulus (MPa)	G_{12}	7540
Poisson's Ratio	ν_{12}	0.15
Axial Strengths (MPa)	X_t	315
	X_c	190
Transverse Strengths (MPa)	Y_t	210
	Y_c	120
Shear Strength (MPa)	S	115
Thermal Expansion Coefficients (1/°C)	α_1	$3.1\ 10^{-6}$
	α_2	$5.5\ 10^{-6}$

mechanical properties of a glass/epoxy composite material used in the problem are given in Table 1. As seen in this table, the composite material shows different properties in the principal material directions. Inner radius of the cylinder, a, is 50 mm. The cylinder is made of four orthotropic layers and each layer has a thickness of 1 mm. Firstly, solutions for only one pressure value are shown, with varying temperatures. Therefore, internal pressure is chosen as 10 MPa, and liquid or gas temperatures (inner temperature), Ta, is taken into consideration for various temperature values such as 20, 50, 110 and 200 °C. Environmental (outer) temperature, Tb, and reference temperature, T_0, are chosen as 20 °C. However, it is assumed that the material properties do not change with increasing temperature. When Ta=20 °C, the cylinder is only subjected to internal pressure. In the situation of only internal pressure, the results obtained for cylinders are in good agreement in comparison with the literature [7, 8]. Then, to observe the true interplay of these stress sources, solutions for multiple pressures and stress distributions for curves of constant Pressure/Temperature ratios are presented.

The radial, tangential and axial stresses in the composite cylinder subjected to internal pressure of 10 MPa at the inner temperature 50 °C are given in Table 2. To see the effects of the wind angle variation through the radial section of the cylinder, the layers are oriented symmetrically and antisymmetrically for (0°/90°), (30°/-30°), (45°/-45°) and (60°/-60°) orientations. Indices "s" and "2" in tables and Figures represent symmetric and antisymmetric orientations, respectively. As seen in this table, radial, tangential and axial stress components of the symmetric and antisymmetric angle-ply cylinders are equal to each other, whereas the stress values of the cross-ply cylinders are different from each other. The radial stress values are equal to inner pressure

Table 2. Stress values at the inner and outer surfaces of the cylinders under P_i=10 MPa and T_a=50 °C, s: Symmetric, 2: Antisymmetric.

Stacking Sequences	At the inner surface			At the outer surface		
	σ_r (MPa)	σ_θ (MPa)	σ_z (MPa)	σ_r (MPa)	σ_θ (MPa)	σ_z (MPa)
$[0°/90°]_s$	-10.00	91.86	9.77	0.00	89.84	13.48
$[0°/90°]_2$	-10.00	91.98	9.79	0.00	111.13	13.49
$[30°/-30°]_s$	-10.00	127.17	31.37	0.00	121.01	33.26
$[30°/-30°]_2$	-10.00	127.17	31.37	0.00	121.01	33.26
$[45°/-45°]_s$	-10.00	112.21	29.74	0.00	108.04	32.11
$[45°/-45°]_2$	-10.00	112.21	29.74	0.00	108.04	32.11
$[60°/-60°]_s$	-10.00	93.88	19.60	0.00	92.15	23.15
$[60°/-60°]_2$	-10.00	93.88	19.60	0.00	92.15	23.15

at the inner surface and zero at outer surface, due to boundary conditions. The tangential and axial stress values at the inner and outer surfaces for (30°/-30°) orientations are higher than that of the other orientations, and the magnitudes of these stress components at the inner surface of the cylinder for all orientations are higher than that of the outer surface. With increasing orientation angle, the stress values are decreasing gradually in both inner and outer surfaces, except for the tangential stress value in the outer surface of antisymmetric cross-ply cylinder. It is found that the stress values for symmetric cross-ply cylinder are minimum.

Through-the-thickness variation of σ_r in the symmetric $[0°/90°]_s$ and antisymmetric $[0°/90°]_2$ cylinders under various temperatures (20, 110 and 200 °C) and internal pressure of 10 MPa is shown in Fig. 3. As seen in this figure, the radial stress components obtained due to the symmetric and antisymmetric stacking sequences are the same up to half of the cylinder thickness, but at the other half of the cylinder thickness they are different from each other. With increasing temperature, although σ_r value for $[0°/90°]_s$ orientation is decreasing step by step, σ_r value for $[0°/90°]_2$ orientation is increasing.

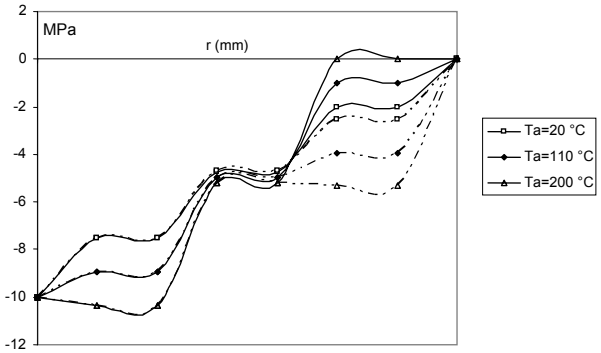

Fig. 3. Through-the-thickness variation of the σ_r in $[0°/90°]_s$ (line) and $[0°/90°]_2$ (dotted line) cylinders

Tangential and axial stress components for $[0°/90°]_s$ and $[0°/90°]_2$ oriented cylinders are shown in Figs. 4 and 5. The tangential stress component changes according to the orientations of layers. When the temperature is increased, the tangential stress values are decreasing. When the temperature is increased further, the tangential stress value at the inner surface decreases further. The axial stress component doesn't changes according to the orientations of layers when the cylinder is only subjected to internal pressure (at T_a=20 °C). But, with increasing temperature, the axial stress component changes according to the orientations of layers, and the axial stress values at the inner region decrease more than that at the outer region.

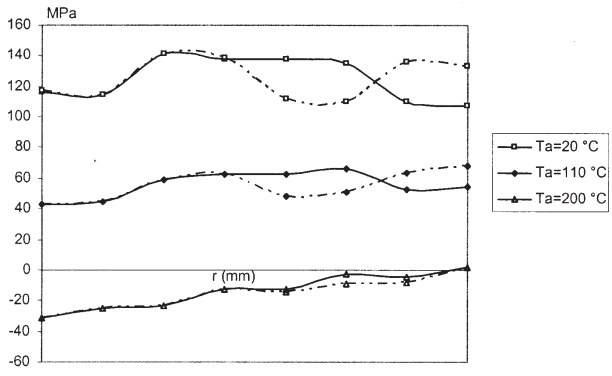

Fig. 4. Through-the-thickness variation of the σ_θ in $[0°/90°]_s$ (line) and $[0°/90°]_2$ (dotted line) cylinders

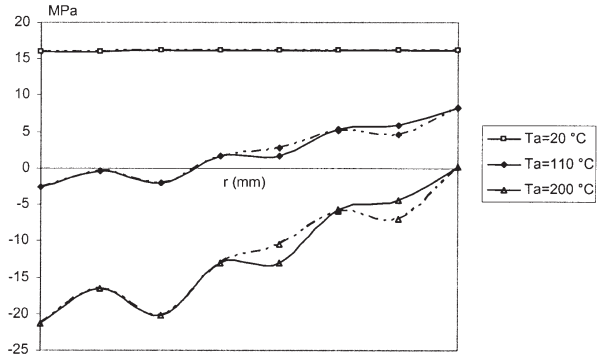

Fig. 5. Through-the-thickness variation of the σ_z in $[0°/90°]_s$ (line) and $[0°/90°]_2$ (dotted line) cylinders

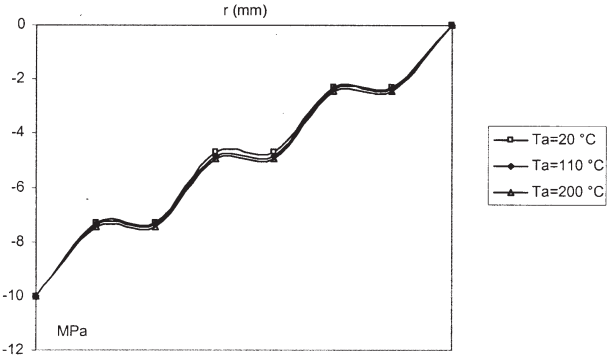

Fig. 6. Through-the-thickness variation of the σ_r in $[30°/-30°]_s$ cylinders

Since the magnitudes of the stress components in

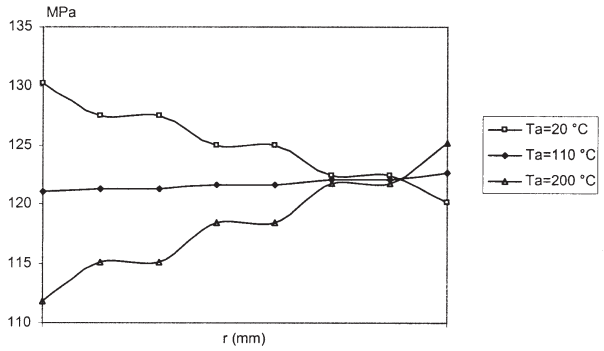

Fig. 7. Through-the-thickness variation of the σ_θ in $[30°/-30°]_s$ cylinders

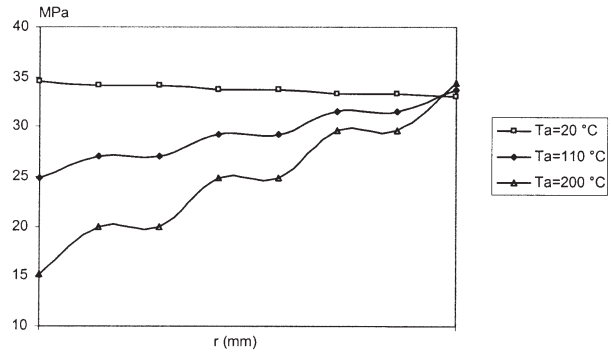

Fig. 8. Through-the-thickness variation of the σ_z in $[30°/-30°]_s$ cylinders

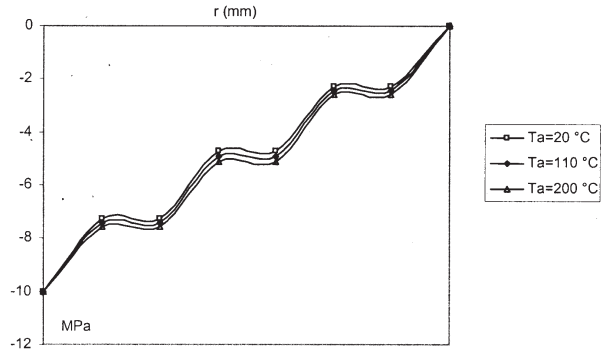

Fig. 9. Through-the-thickness variation of the σ_r in $[45°/-45°]_s$ cylinders

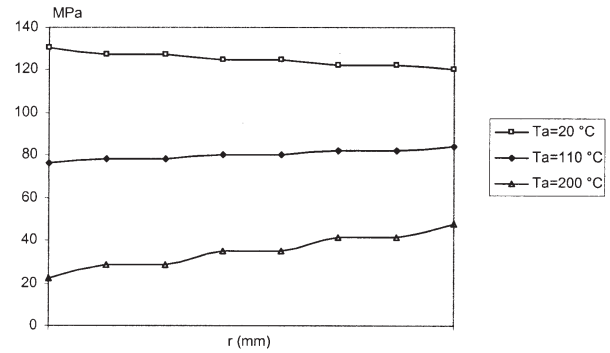

Fig. 10. Through-the-thickness variation of the σ_θ in $[45°/-45°]_s$ cylinders

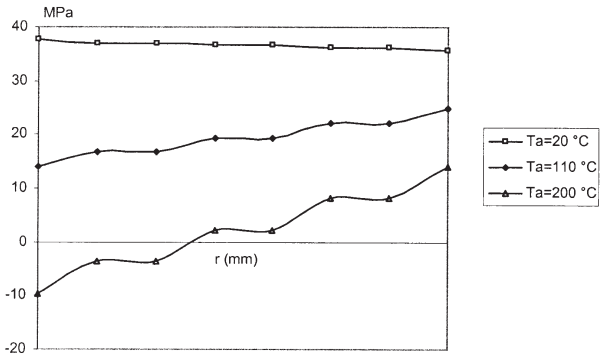

Fig. 11. Through-the-thickness variation of the σ_z in $[45°/-45°]_s$ cylinders

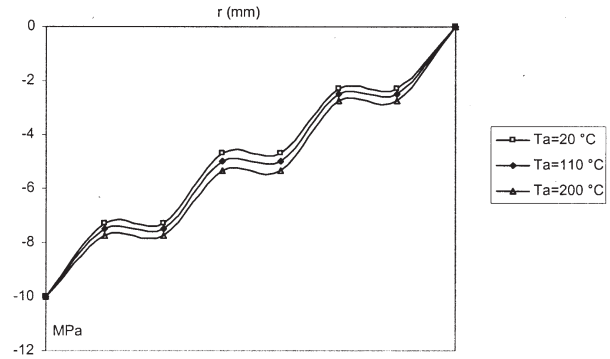

Fig. 12. Through-the-thickness variation of the σ_r in $[60°/-60°]_s$ cylinders

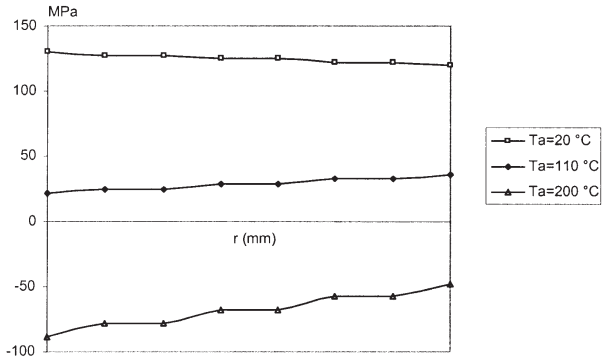

Fig. 13. Through-the-thickness variation of the σ_θ in $[60°/-60°]_s$ cylinders

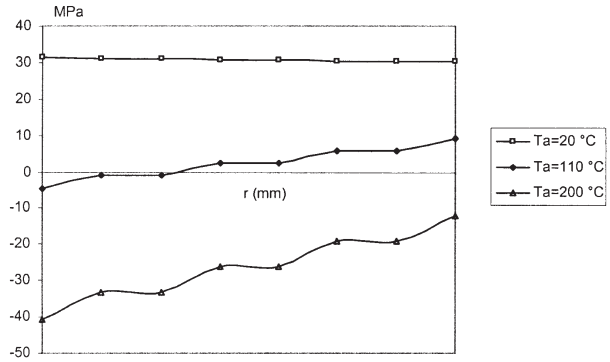

Fig. 14. Through-the-thickness variation of the σ_z in $[60°/-60°]_s$ cylinders

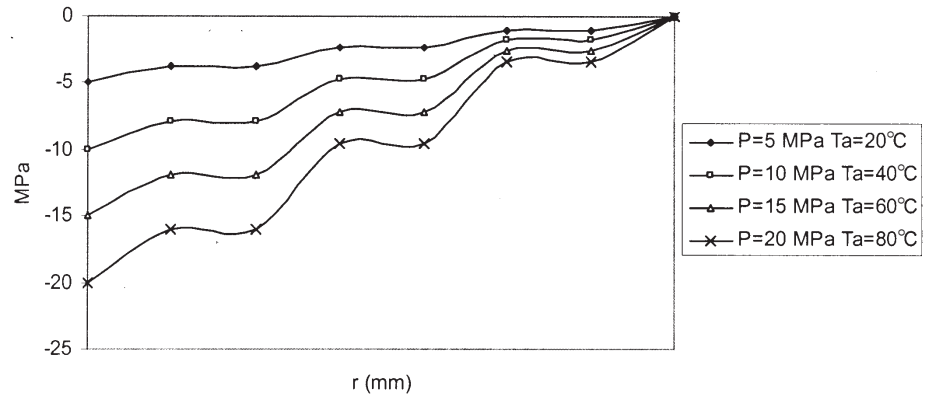

Fig. 15. Through-the-thickness variation of the σ_r in $[0°/90°]_s$ cylinders

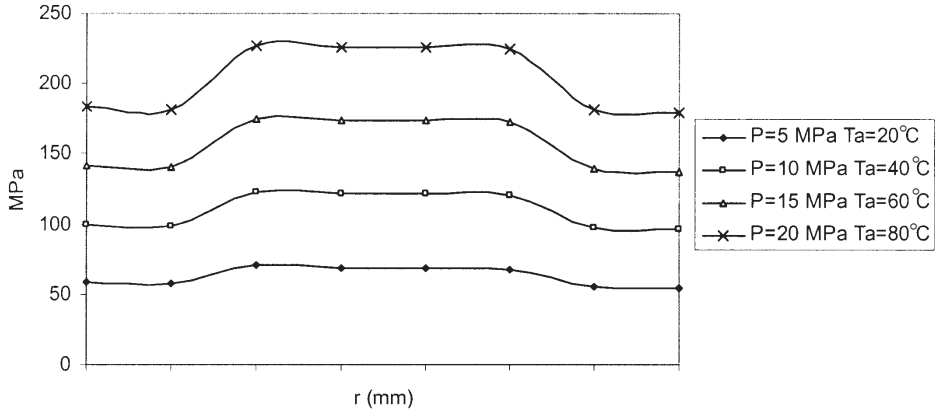

Fig. 16. Through-the-thickness variation of the σ_θ in $[0°/90°]_s$ cylinders

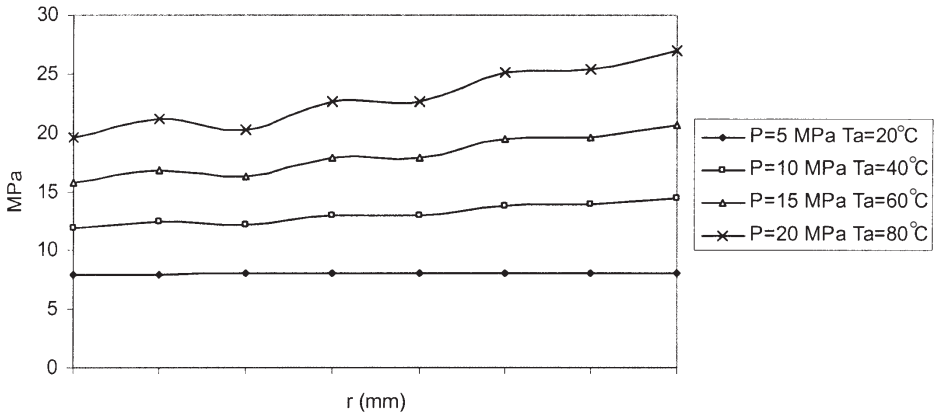

Fig. 17. Through-the-thickness variation of the σ_z in $[0°/90°]_s$ cylinders

the symmetric and antisymmetric angle-ply cylinders are the same, distributions of the stress components in the symmetric angle-ply cylinders are merely shown in Fig. 6 shows through-the-thickness variation of the σr in $[30°/-30°]_s$ cylinders. With increasing temperature, variation of the radial stresses doesn't change further. The radial stress values at the inner surface and outer surfaces are equal to internal pressure and zero, respectively.

Figs. 7 and 8 show through-the-thickness variations of the σ_θ and σ_z in $[30°/-30°]_s$ oriented cylinders. When the cylinder is only subjected to internal pressure, the magnitudes of σ_θ and σ_z at the inner surface are higher than that at the outer surface. When the temperature is increased further, the tangential and axial stress values at the inner surface decrease further, however, the stress values at the outer surface increase very little.

Variations of the radial, tangential and axial stress components for symmetric [45°/-45°]s and [60°/-60°]s oriented cylinders are shown in Figs. 9-14, respectively, and they are similar to [30°/-30°]s cylinder. When the both orientation angle and temperature are increased, the variation of the radial stresses changes very little whereas, the variations of the tangential and axial stresses change further in comparison with the stresses in [30°/-30°]s oriented cylinder. With increasing temperature, the distributions of the tangential and axial stresses are slightly decreasing, as shown in Figs. 10 and 11, 13 and 14.

Drastic reductions in magnitude of the tangential and axial stresses are seen as temperature increases. Solutions for multiple pressures and stress distributions for curves of constant Pressure/Temperature ratios are considered to observe how these trends/ changes are affected if pressure is again increased and the true interplay of these stress sources. Pressure/Temperature ratio is considered as 1/4 when Pi= 5, 10, 15 and 20 MPa, temperature T_a=20, 40, 60 and 80 °C. The solution for only $[0°/90°]_s$ oriented cylinder is presented, and σ_r, σ_θ and σ_z stress distributions for curves of Pi/Ta =1/4 are depicted in Figs. 15, 16 and 17. When both internal pressure and inner temperature are increased, the magnitude of σ_r is equal to inner pressure at the inner surface, but σ_r, σ_θ and σ_z stress distributions at intersection of $[0°/90°]_s$ oriented cylinder are fluctuated. σ_θ values at the inner and outer surfaces are about equal to each other, whereas σ_z values are increased more at outer surface than at the inner surface.

5. CONCLUSIONS

In this study, a stress analysis is developed for multilayered composite thick or thin cylinders. The solution is carried out for plane-strain case.

1. The radial, tangential and axial stress components change according to the orientations of layers in the cross-ply oriented cylinders, whereas the stresses don't change for symmetric and antisymmetric angle-ply oriented cylinders.
2. With increasing temperature, the tangential and axial stress values decrease more at the inner surface than at the outer surface, expect for $[30°/-30°]_s$ cylinder.
3. When the cylinder is subjected only to internal pressure, the magnitudes of σ_θ and σ_z at the inner surface are higher than those at the outer surface for angle-ply cylinders. Then, when temperature is increased, the magnitudes of σ_θ and σ_z at the inner surface are decreasing slightly as to those at the outer surface.
4. When both internal pressure and inner temperature increase (P_i/T_a=1/4), σ_r, σ_θ and σ_z stress distributions at intersection of $[0°/90°]_s$ oriented cylinder fluctuate more than that at the former pressure and temperature.
5. σ_θ values at the inner and outer surfaces are about equal to each other, whereas σ_z values are increasing more at outer surface than those at the inner surface.

References:

1. **Lekhnitskii S.G.** "Theory of Elasticity of an Anisotropic Body" Mir Publishers, Moscow, (1981), 215-237.
2. **Rosenow, M.W.K.** "Wind angle effects in glass fibre-reinforced polyester filament wound pipes", *Composites,* **15** (1984), 144-152.
3. **Hyer, M.J., Cooper, D.E and Cohen, D.** " Stress and deformation in crossply composite tube subjected to uniform temperature change", *Journal of Thermal Stresses,* **9** (1986), 97-117
4. **Soden, P.D., Kitching, R., Tse, P.C., Hinton, M.J. and Tsavalas, Y.** "Influence of Winding Angle on The Strength and Deformation of Filament-Wound Composite Tubes Subjected to Uniaxial and Biaxial Loads" *Composites Science and Technology,* **46**/4 (1993), 363-378.
5. **Chouchaoui, C.S. and Ochoa, O.O.** "Similitude study for a laminated cylindrical tube under tensile, torsion, bending, internal and external pressure. Part I: Governing equations", *Composite Structures,* **44** (1999), 221-229.
6. **Xia, M, Takayanagi, H. and Kemmochi, K.** "Analysis of Transverse Loading for Laminated Cylindrical Pipes", *Composite Structures,* **53** (2001), 279-285.
7. **Xia, M, Takayanagi, H. and Kemmochi, K.** "Analysis of Multi-Layered Filament-Wound Composite Pipes Under Internal Pressure), *Composite Structures,* **53** (2001), 483-491.
8. **Wild, PM, Vickers, GW.** "Analysis of Filament-Wound Cylindrical Shells Under Combined Centrifugal, Pressure And Axial Loading", *Composites Part A,* **28A** (1997), 47-55.
9. **Chen, T., Chung, C.T. and Lin, W.L.** "A revisit of a cylindrically anisotropic tube subjected to pressuring, shearing, torsion, extension and a uniform

temperature change" *Int. J. of Solid and Structures*, **37** (2000), 5143-5159.

10. **Tarn, J.Q. and Wang, Y.M.** "Laminated composites tubes under extension, torsion, bending, shearing and pressuring: a state space approach", *Int. J. of Solid and Structures,* **38** (2001), 9053-9075.
11. **Xia, M., Takayanagi, H. and Kemmochi, K.** "Bending Behaviour of Filament-Wound Fibre-Reinforced Sandwich Pipes", *Composite Structures,* **56** (2002), 201-210.
12. **Xia, M., Kemmochi, K. and Takayanagi, H.** "Analysis of Filament-Wound Fibre-Reinforced Sandwich Pipe under Combined Internal Pressure and Thermomechanical Loading", *Composite Structures,* **51** (2001), 273-283.
13. **Liew, K.M., Kitipornchai, S., Zhang, X.Z. and Lim, C.W.** "Analysis of the thermal stress behaviour of functionally graded hollow circular cylinders", *Int. J. of Solid and Structures,* **40** (2003), 2355-2380.
14. **Sayman, O.** (2005). "Analysis of multi-layered composite cylinders under hygrothermal loadings", *Composite: Part A,* **36:** 923-933.
15. **Parnas, L. and Katırcı, N.** "Design of Fibre-Reinforced Composite Pressure Vessels under Various Loading Conditions", *Composite Structures,* **58** (2002), 83-95.
16. **Beakou, A. and Mohamed, A.** "Influence of Variable Scattering on the Optimum Winding Angle of Cylindrical Laminated Composites", *Composite Structures,* **53** (2001), 287-293.
17. **Kaddour, A.S, Hinton, M.J and Soden, P.D.** "Behaviour of $\pm$45° Glass/Epoxy Filament Wound Composite Tubes under Quasi-Static Equal Biaxial Tension-Compression Loading: Experimental Results", *Composites Part,* **34** (2003), 689-704.
18. **Mistry, J, Gibson, A.G and Wu, Y.S.** "Failure of Composite Cylinders Under Combined External Pressure and Axial Loading", *Composite Structures,* **22**/4 (1992), 193-200.
19. **Tarakçıoğlu, N., Akdemir, A. ve Avcı, A.** "Strength of Filament Wound Grp Pipes with Surface Crack", *Composites Part B,* **32** (2001), 131-138.
20. **Çallıoğlu, H.** "Stress Analysis of an Orthotropic Rotating Disc under Thermal Loading", *J. of Reinforced Plastics and Composites;* **23**/17 (2004), 1859-1867.